TWENTYFIFTH EUROPEAN ROTORCRAFT FORUM

Paper n° P6

FLIGHT EVALUATION OF AN ADAPTIVE NEURAL NETWORK FLIGHT CONTROLLER OF AN UNINHABITED HELICOPTER

BY

A.J. CALISE J.V.R. PRASAD J.E. CORBAN

GEORGIA INSTITUTE OF TECHNOLOGY GUIDED SYSTEMS TECHNOLOGIES, INC.

USA

SEPTEMBER 14–16, 1999
ROME
ITALY

ASSOCIAZIONE INDUSTRIE PER L' AEROSPAZIO, I SISTEMI E LA DIFESA
ASSOCIAZIONE ITALIANA DI AERONAUTICA ED ASTRONAUTICA

Flight Evaluation of an Adaptive Neural Network Flight Controller of an Uninhabited Helicopter

A. J. Calise
Professor

J.V.R. Prasad
Professor

School of Aerospace Engineering
Georgia Institute of Technology
Atlanta, GA 30332-0150, USA

J.E. Corban
President
Guided Systems Technologies, Inc.
P.O. Box 1453
McDonough, GA 30253, USA

Abstract

This paper presents recent results from our experimental flight controls research program, which is presently focused on flight evaluation of a neural network-based adaptive flight controller. A description is given of the uninhabited helicopter flight controls research testbed and associated avionics package. This is followed by a detailed description of our adaptive neural network-based flight control architecture for attitude and trajectory control. The paper concludes with results from our simulation and flight experiments.

1. Introduction

Traditional methods of flight control design consist of gain scheduling many linear point designs across the flight envelope using a high fidelity dynamic simulation. Continued reliance on these (albeit proven) methods contributes greatly to the expense associated with producing a new flight vehicle, and also limits achievable system performance. This is especially true when the flight system dynamics exhibit strong nonlinearities or are uncertain.

As an alternative, nonlinear techniques such as feedback linearization and dynamic inversion have been developed. Despite the power of these techniques, they fail to produce truly significant economic or performance-based improvements due to continued dependence on precise knowledge of the system dynamics. Research at Georgia Tech has recently demonstrated a direct neural network-based adaptive control architecture that can compensate for unknown plant nonlinearities in a feedback linearizing setting. These neural network-based controllers look very much like traditional adaptive control elements. Neural networks are viewed as highly nonlinear control elements that offer distinct advantage over more conventional linear parameter adaptive control elements in achieving system performance.

In order to experimentally validate our research, and to support other activities in the area of autonomous flight vehicles research, we have developed an experimental flight controls research facility using a Yamaha R-50 uninhabited helicopter. The objective of this paper is to present an overview of our neural network-based adaptive control methodology, describe the flight controls research test bed, and then summarize some of our simulation and flight test results.

2. Uninhabited Aerial Vehicle Research Facility

The Uninhabited Aerial Vehicle Research Facility (UAVRF) was initiated in June of 1997. This facility is dedicated to flight testing of advanced control algorithms on uninhabited helicopters. It presently contains two Yamaha model R-50 helicopters, each having 12 HP liquid cooled engines, a payload capability of 44 pounds and endurance of approximately 30 minutes.

The on-board system consists of a 200 Mhz Pentium-based flight control processor with 32 Mb RAM and an R-1 integrated avionics system. The list of on-board sensors includes: Boeing DQI-NT Inertial Measuring Unit, NovTel RT-2 differential GPS with 2 cm accuracy, 3-axis magnetometer, and 8 channel ultrasonic ranging system. A wireless modem digital data link is used to provide a two way communication link with a mission control ground station. In addition, an on-board multiplexer switch allows a human safety pilot to engage the system, and to over-ride the flight control system in the event of an emergency. The control actuators consist of 3 linear servos for cyclic and collective controls, and 2 rotary servos for yaw and throttle controls. The UAVRF also houses two 300Mhz PCs that are used for hardware in the loop simulation, which permits accurate simulation and hardware testing of each mission prior to flight test.

3. Simulation Model

A nonlinear simulation model of the R-50 helicopter has been developed based on the math model given in Ref. 1. The model of Ref. 1 includes, in addition to a six degrees-of-freedom fuselage, a first-order representation of main rotor flapping and quasi-steady representation of main and tail rotor inflows. This model has been modified to include a simplified control rotor model developed in Ref. 2, a pilot's radio controller model and simplified engine and RPM governor models. Initial estimates of the aerodynamic data are adjusted using flight test data.

4. Adaptive Nonlinear Flight Control

This section presents an overview of the control system design.[3, 4] The interested reader is referred to the cited references for more background on the subject approach to direct adaptive control of nonlinear systems, additional design details, derivation of the neural network update law, and a proof of stability.

4.1 Attitude/Rate Command Controller

The controller can be configured in each of the three rotational axes independently as either an attitude or a rate command system. Handling qualities are prescribed by the use of command filters which serve both to limit the input rate, and as a model for desired response. Specification of "good" handling qualities is not yet well defined for uninhabited helicopters, and is the subject of future research. Figure 1 presents a block diagram of the control system architecture for the longitudinal channel when this channel is configured for attitude command. The lateral and directional channels are identical in form. The construction of this block diagram is discussed in the following.

The design starts with an approximate linear model of the rotational dynamics of the helicopter, which is to be inverted at a nominal operating condition.

$$\ddot{\Theta} = A_1 x_1 + A_2 \omega + B_1 \delta_{COL} + B_2 \delta \qquad (1)$$

In Eq. (1), $\Theta = [\phi\ \theta\ \psi]^T$ is the vector of body attitudes, $\omega = [p\ q\ r]^T$ is the vector of angular rates about the body fixed axes[5], and A_1, A_2, and B_1, B_2 represent matrices of the aerodynamic stability and control derivatives at the nominal operating point, respectively. The vector of standard helicopter control inputs, δ, is employed. It contains lateral and longitudinal cyclic pitch, δ_{LAT} and δ_{LON}, and tail rotor collective pitch, δ_{DIR}. The vector x_1 consists of body axis velocity components of the vehicle mass center. In this formulation, the main rotor collective control position, δ_{COL}, is taken to be prescribed by an outer loop trajectory controller or by a human operator.

The methodology assumes the 'pseudo control' vector, U, to be of the form

$$U = U_c - U_{AD} \qquad (2)$$

The elements of U_c are the outputs of independent linear controllers, each operating on its corresponding error signal. The linear controller designs are used to specify the tracking error transients in each channel. Typically the transient is designed to be fast relative to the dynamics of the command filter but slow relative to the actuator dynamics. In the attitude command system shown in Fig. 1,

$$U_c = K_p(\theta_c - \theta) + K_d(\dot{\theta}_c - \dot{\theta}) + \ddot{\theta}_c \qquad (3)$$

where θ denotes the pitch Euler angle[5]. In this case a second order command filter is employed, and the second time derivative of the command is fed forward.

The left-hand side of Eq. (1) is set equal to the pseudo controls constructed for each channel. The result is then solved for the vector of helicopter controls

$$\delta = B_2^{-1}\{U - A_1 x_1 - A_2 \omega - B_1 \delta_{COL}\} \qquad (4)$$

Note that the linear model being inverted is only an approximation to the true helicopter dynamics, and that inversion error will therefore result in each channel. This inversion error can be expressed as a function of the states and pseudo controls.

The neural network output, U_{AD}, serves to adaptively cancel these inversion errors through on-line learning. The learning is accomplished by a simple weight update rule derived from Lyapunov theory, thus assuring ultimate boundedness of the response of the closed-loop system. The subject design employs a multi-layer neural network with sigmoidal activation functions in the hidden layer. A neural network of this type is capable of approximating any smooth function to any desired accuracy, provided the number of hidden layer neurons is sufficiently large. Inputs to the neural network in each channel are taken as rotational states, pitch and roll Euler angles, and the corresponding pseudo control.

In some piloting tasks, one may prefer instead a rate command system. In such a case, integral action is added in the linear controller to provide for attitude retention giving it the designation Rate Command, Attitude Hold (RCAH).

4.2 Trajectory Tracking Controller

A trajectory controller is designed to form an outer loop to the attitude command system described in the previous subsection. The relationship between the components of acceleration of the vehicle mass center and components of external forces acting on the vehicle can be expressed as

$$\begin{bmatrix} \ddot{X} \\ \ddot{Y} \\ \ddot{Z} \end{bmatrix} = L_{Vb}(\phi,\theta,\psi)\begin{bmatrix} F_x/m \\ F_y/m \\ F_z/m \end{bmatrix} + \begin{bmatrix} 0 \\ 0 \\ g \end{bmatrix} \qquad (5)$$

where X, Y and Z are the position components of the vehicle mass center in the earth-fixed (North, East, Down) coordinate system, L_{Vb} is the transformation matrix from body axes to earth-fixed axes, ϕ, θ *and* ψ are the Euler roll, pitch and yaw attitudes, respectively, F_x, F_y and F_z are total aerodynamic force components along the body axes, m is vehicle mass and g is the constant of acceleration due to gravity. Following the trajectory controller synthesis described in[6,7], a set of pseudo-controls, $U_1, U_2, and\ U_3$, are formulated as

$$U_1 = K_x(X_c - X) + K_{\dot{x}}(\dot{X}_c - \dot{X}) + \ddot{X}_c \qquad (6)$$

$$U_2 = K_y(Y_c - Y) + K_{\dot{y}}(\dot{Y}_c - \dot{Y}) + \ddot{Y}_c \qquad (7)$$

$$U_3 = K_z(Z_c - Z) + K_{\dot{z}}(\dot{Z}_c - \dot{Z}) + \ddot{Z}_c \qquad (8)$$

where the subscript c denotes commanded value. Next, the left-hand side of Eq. (5) is replaced by the values of the pseudo-controls U_1, U_2 and U_3 computed from Eqs. (6)~(8). This will result in a set of algebraic equations which can be rearranged as

$$\begin{bmatrix} U_1 \\ U_2 \\ U_3 - g \end{bmatrix} = L_{Vb}(\phi,\theta,\psi)\begin{bmatrix} F_x/m \\ F_y/m \\ F_z/m \end{bmatrix} \qquad (9)$$

Equation (9) can be used to compute the values of pitch and roll attitudes required for horizontal (both X and Y position, velocity and acceleration) command tracking. In the process, certain approximations are made in order to simplify the resulting computations.

First, the magnitudes of cyclic and pedal control forces are assumed to be much smaller compared to the collective control force and hence, they are neglected. Second, the F_x and F_y (i.e., body x-axis and y-axis aerodynamic force components) are assumed to be small in magnitude compared to F_z (body z-axis force component) and hence, they are neglected in Eq. (9). With these approximations, closed-form expressions for the required pitch and roll attitudes can be obtained as

$$\bar{\theta} \approx \tan^{-1}\left(\frac{U_1\cos\Psi_c + U_2\sin\Psi_c}{U_3 - g}\right) + \theta_{trim} \qquad (10)$$

$$\bar{\phi} \approx \sin^{-1}\left(\frac{-U_1\sin\Psi_c + U_2\cos\Psi_c}{\sqrt{U_1^2 + U_2^2 + (U_3 - g)^2}}\right) + \phi_{trim} \qquad (11)$$

where $\bar{\phi}$ and $\bar{\theta}$ are the required roll and pitch attitudes, respectively, and ψ_c is the commanded yaw attitude. The values of $\bar{\phi}$ and $\bar{\theta}$ computed using Eqs. (10) and (11) along with ψ_c are used as command inputs to the inner loop attitude control system shown in Fig.1, which in turn will determine inputs to the cyclic and pedal control actuators.

4.3 Determination of Collective Control

Taking magnitude of both sides of Eq. (9) results in

$$A = \sqrt{U_1^2 + U_2^2 + (U_3 - g)^2} \qquad (12)$$

where A is the specific aerodynamic force magnitude which can be measured using a three-axis accelerometer measurement unit.

With the assumption that the specific aerodynamic force magnitude is primarily affected by the collective control, a simple linear controller[7] can be synthesized so as to satisfy Eq. (12). Denoting the right hand side of Eq. (12) as A_c, the integrated value of the difference between A_c and A is used to adjust the collective control. A block diagram representation of the overall controller is shown as Fig. 2 wherein the controller is configured to include only horizontal velocity commands (V_{Xc} and V_{Yc}), vertical position command (Z_c), and yaw attitude command ψ_c. The horizontal velocity commands are passed through first-order filters and the altitude command is passed through a second-order filter in order to limit command rates and to achieve prescribed desired handling qualities. Also, the magnitudes of U_1 and U_2 are limited to be within 0.5g and the upper bound of U_3 is limited to be less than 0.5g. to avoid very large excursions in the computed values of required pitch and roll attitudes.

5. Control System Implementation

For the purpose of real-time simulation and flight test, the control system formulation presented in the previous section has been coded in the C programming language. It runs in real-time in double precision with an update rate of 100 Hz on a 200 MHz Pentium-based Single Board Computer (SBC). The SBC is interfaced via shared memory to a previously developed commercial-grade flight control system known as the R1. The R1 provides for collection and management of sensor data, hardware and software interface to both the actuators and the pilot, and management of all telemetry links to a ground control station. For the current program, the R1 flight control system with SBC has been integrated on a Yamaha R-50 industrial uninhabited helicopter, which is a 150 pound gross weight production vehicle designed for agricultural spraying. The result is a very capable uninhabited helicopter test bed. Features of the R1 flight control system and its sensor suite are discussed in the following.

The R1 system is designed to support the integration of independent functional modules in order to accommodate a wide variety of research needs. Up to four Motorola 68332 processors communicate using high speed serial data transmissions (Motorola Queued Serial Peripheral Interface, QSPI). There are two 16 channel 12 bit analog to digital conversion boards interfaced to the primary 68332 via the QSPI. The four 68332s provide a total of 64 digital input/output channels with precision timing control functions for tasks such as generation and reading of pulse code modulated signals.

The R1 card cage also houses driver circuitry for an eight channel ultrasonic ranging system. This system is used to measure range to the ground over prepared surfaces during take-off and landing sequences. The card cage also accommodates a spread spectrum digital data link and a NovTel RT-2 differential GPS receiver (2 cm accurate position sensing in differential mode with carrier phase lock and 5 Hz update rate). The GPS system is integrated with a Boeing DQI-NT Inertial Measuring Unit (IMU) with a complete GPS-aided inertial navigation solution. The system has a 12 channel interface to standard pulse width modulated radio control equipment for the pilot interface, and sensors for measuring the rotational rates, temperatures, etc. The system operates on a 12 to 28V DC input power supply.

6. Flight Evaluations of ACAH

The inverting controller design allows for the error dynamics characteristics to be prescribed, along with a proportional and a derivative gain. The gains were computed from specified values of damping and natural frequency as follows:

$$K_d = 2\zeta\ \omega_n$$

$$K_p = \omega_n^2$$

The inverting controller design is based upon inversion of a linear model of the helicopter in hover using only the matrix parameters along the diagonal identified from flight tests.

Flight test results for the pitch channel ACAH controller are presented in Figures 3 through 6. Only the pitch channel ACAH controller was used in this case. First, the gains in the linear part of the inverting controller with the network turned off were tuned during flight for achieving acceptable command tracking performance from the controller. The controller gains were varied such that the damping ratio was set at 0.8 while the natural frequency varied from 1 to 3 rad/sec. Figure 3 shows the effect of varying controller gains on the attitude tracking performance in the pitch channel with the neural network turned off wherein the damping ratio was set at 0.8 while the natural frequency was varied from 2 to 3 rad/sec. The highest natural frequency case can be found between 2545 and 2580 time step numbers where slightly unstable oscillation occurred. The observed instability at higher controller gain was attributed to significant time delays in the data acquisition system. To prevent the instability caused by high gain, the natural frequency was selected as ω_n=2.0 rad/sec. Next, with the neural network turned on, the weight update rate (assumed to be same for the output layer weights and the hidden layer weights for convenience) was tuned during flight. Figure 4 shows the effect of varying weight update rate with the previously selected values of damping ratio ζ=0.8 and natural frequency ω_n = 2 rad/sec. The weight update rate was 8 at the time step number 5200 and unstable oscillations were observed around the time step number 5420 with the weight update rate at 20. From these results, the weight update rate was set at 15 for further evaluations of the adaptive neural net controller for the pitch channel.

Figures 5 and 6 show the performance of the pitch channel controller without and with neural network

adaptation, respectively, for typical doublet commands. Significant improvements in command tracking performance are noticed with neural net adaptation (Fig. 6) as compared to that without neural network (Fig. 5). It is felt that further improvements in controller performance can only be achieved with an increase of controller bandwidth, which currently is limited by the significant time delays present in the data acquisition system. Work is currently in progress for ways of improving the controller bandwidth in the pitch channel.

Figures 7 through 9 show the flight test results of the roll channel ACAH controller case. Steps similar to the pitch channel case were used for adjusting the controller gains and network update rate for the roll channel controller. Similar to the pitch channel case, instability was observed when the controller gains with the network turned off were increased as shown in Fig. 7. A slightly higher bandwidth could be achieved in the roll channel as compared to the pitch channel before instability was observed due to the effect of inherent time delays in the data acquisition system. However, it is felt that the roll channel bandwidth is still low and work on further improving the controller bandwidth is currently in progress.

Figures 8 and 9 show the roll channel controller performance without and with neural network adaptation, respectively, with the controller gains set for ζ=0.8 and ω_n=3.5 rad/sec and the network weight update rate set at 45. A significant improvement in controller performance can be seen with neural network adaptation (Fig. 8) as compared to the case without the neural network (Fig. 9).

7.Simulation Results (Trajector Controller)

An initial evaluation of the performance of the trajectory controller was carried out using a nonlinear simulation model of the Yamaha R-50 helicopter.[7, 8] The initial evaluation was carried out without inclusion of any time delay effects. The following values of controller gains were used:

$$K_{\dot{x}} = 0.5, K_{\dot{y}} = 0.5,\ K_z = 0.187, K_{\dot{z}} = 1.87, K_a = 15$$

$$\begin{array}{lll} \textit{Pitch loop}: & K_\theta = 100 & K_{\dot{\theta}} = 16 \\ \textit{Roll loop}: & K_\phi = 225 & K_{\dot{\phi}} = 24 \\ \textit{Yaw loop}: & K_\psi = 100 & K_{\dot{\psi}} = 16 \end{array}$$

The command trajectory, as shown in Fig. 10, consisted of vertical climb, hover, forward flight, sideward flight, backward flight, a part of elliptical turn, and landing. Simulation results of trajectory tracking and control variations are shown in Figs. 11 and 12, respectively. From these initial evaluations, it can be seen that the trajectory controller performance is quite good. Further simulation evaluations with realistic time delay effects and flight test evaluations of the trajectory controller are currently in progress.

8. Summary

Design of a helicopter control system using a combination of feedback linearization and a neural network-based technique for on-line adaptation is presented. Hardware and software implementation of the controller on an unmanned helicopter testbed is then discussed. Simulation as well as flight test evaluation results are presented to illustrate the improvements in controller performance with adaptive neural networks. Work is currently in progress on how to further improve the performance of the adaptive neural net controller and flight test evaluations of the trajectory controller.

9. Acknowledgements

This work is supported in part by the U.S. Army Research Office under Contract NCC 2-945, and in part by the U.S. Army Aerostructures Directorate, Contract NAS1-20313.

The authors would like to acknowledge the dedicated efforts of Research Engineers Jeong Hur and Robert Pickell of Georgia Tech and GST, respectively, as well as the invaluable contributions of the following Georgia Tech graduate students (in alphabetical order) Eric Johnson, Suresh Kannan, Seungjae Lee, Christian Munzinger, Yubo Pei, Rolf Rysdyk and Manu Sharma.

10. References

1. Heffley, R. K., M. A. Mnich, "Minimum-Complexity Helicopter Simulation Model Math Model, NASA CR-177476, USAAVSCOM Technical Report 87-A-7, April 1988.
2. Perhinschi, M. and Prasad, J.V.R., "A Simulation Model of an Autonomous Helicopter," Proceedings of the RPV/UAV Systems 13th Digital International Conference, April 1998.
3. Calise, A. J. and R. T. Rysdyk, "Nonlinear Adaptive Flight Control Using Neural Networks", IEEE Control Systems Magazine, Vol.18, No.6, pp.14-25, December 1998.
4. McFarland, M. B., and A. J. Calise, "Multilayer Neural Networks and Adaptive Nonlinear Control

of Agile Anti-Air Missiles", Proceedings of the AIAA Guidance, Navigation and Control Conference, Paper No. AIAA 97-3540, August 1997.

5. Etkin, Bernard, Dynamics of Atmospheric Flight, 1972, John Wiley & Sons, Inc.
6. Prasad, J.V.R. and Lipp, A.M., "Synthesis of a Helicopter Nonlinear Flight Controller Using Approximate Model Inversion", Mathl. Comput. Modelling Vol. 18, No.3-4, pp. 89-100, 1993.
7. Prasad, J.V.R., Calise, A.J., Pei, Y. and Corban, J.E., "Adaptive Nonlinear Controller Synthesis and Flight Test Evaluation on an Unmanned Helicopter," Proceedings of the IEEE Conference on Control Applications, Hawaii, August 1999.
8. Corban, J.E., Calise, A.J. and Prasad, J.V.R., "Implementation of Adaptive Nonlinear Control for Flight Test on an Unmanned Helicopter", Proceedings on the 37th IEEE Conference on Decision & Control, 1998.

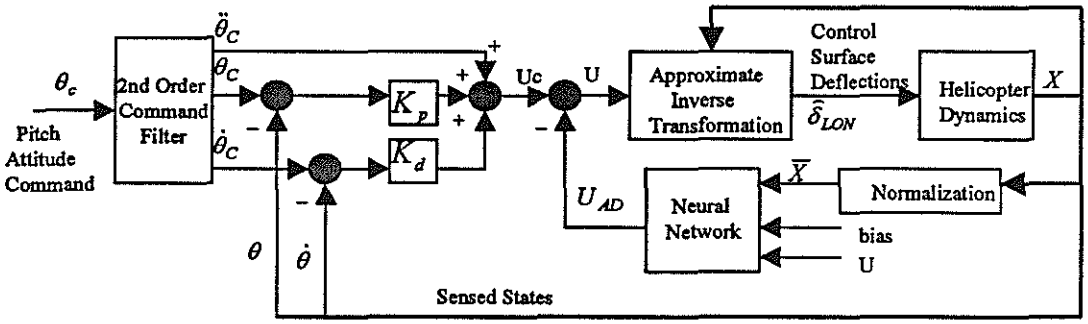

Figure 1. Block diagram of Attitude Command, Attitude Hold (ACAH) system for pitch channel.

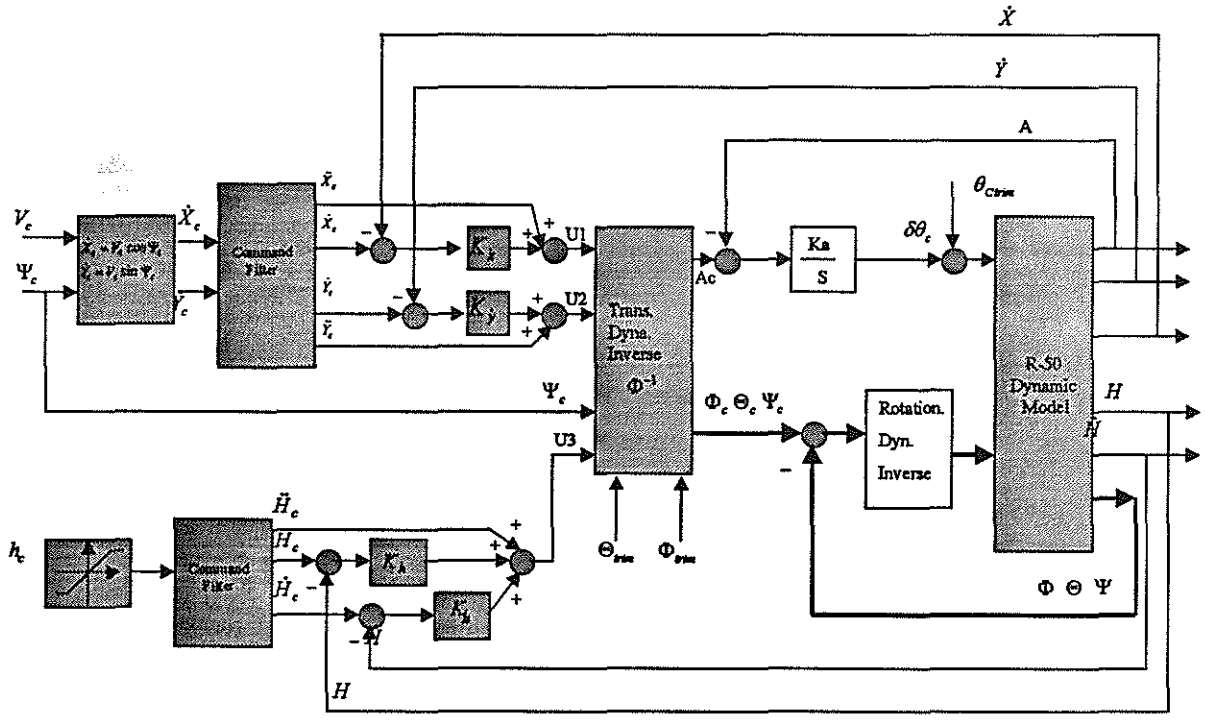

Figure 2. Block diagram of trajectory controller.

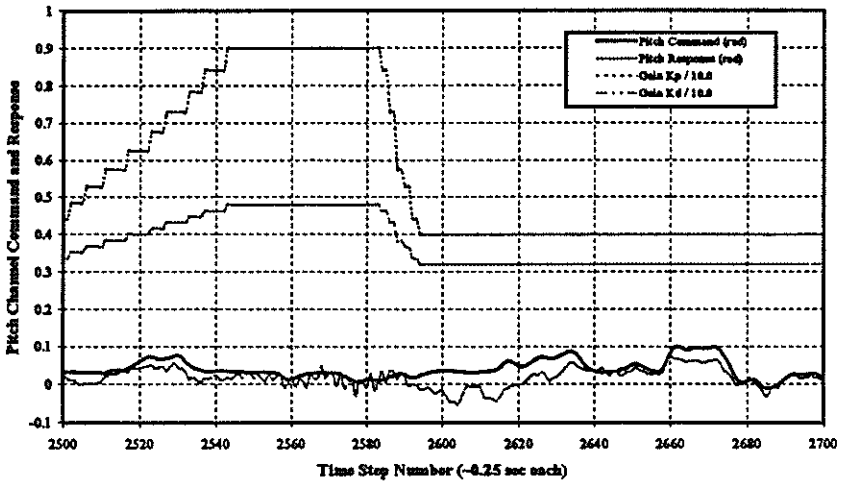

Figure 3. Pitch ACAH response, $\zeta = 0.8$, ω_n is varied from 2 to 3 rad/sec, no neural network.

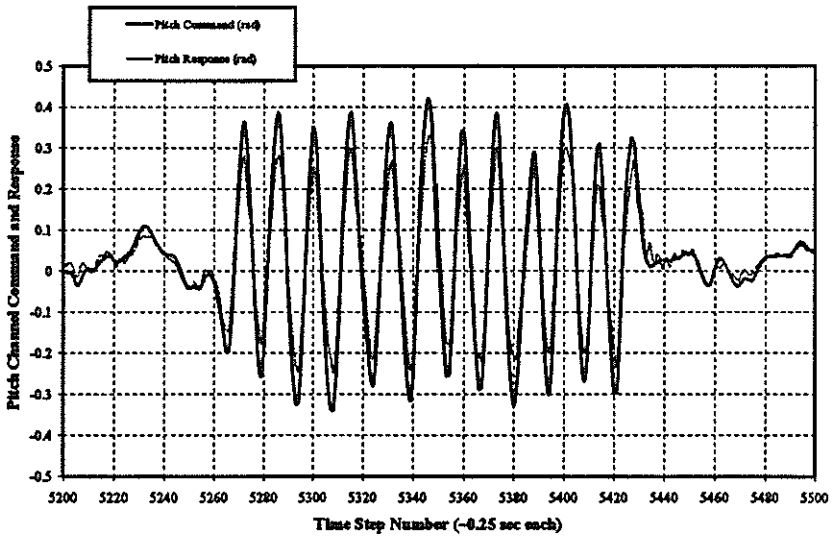

Figure 4. Pitch ACAH response, $\zeta = 0.8$, $\omega_n = 2.0$ rad/aec, with NN adaptation rate varied from 8 to 20.

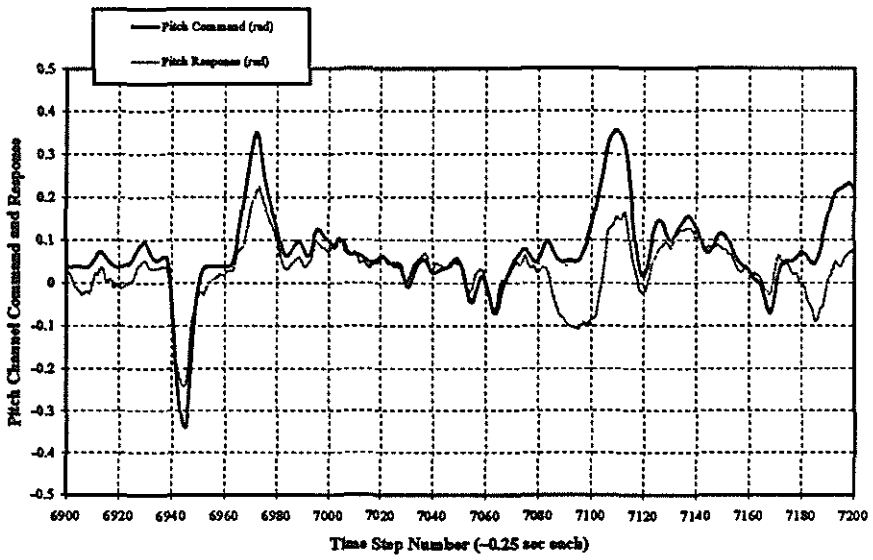

Figure 5. Pitch ACAH response for a doublet command, $\zeta = 0.8$, $\omega_n = 2.0$, no neural network.

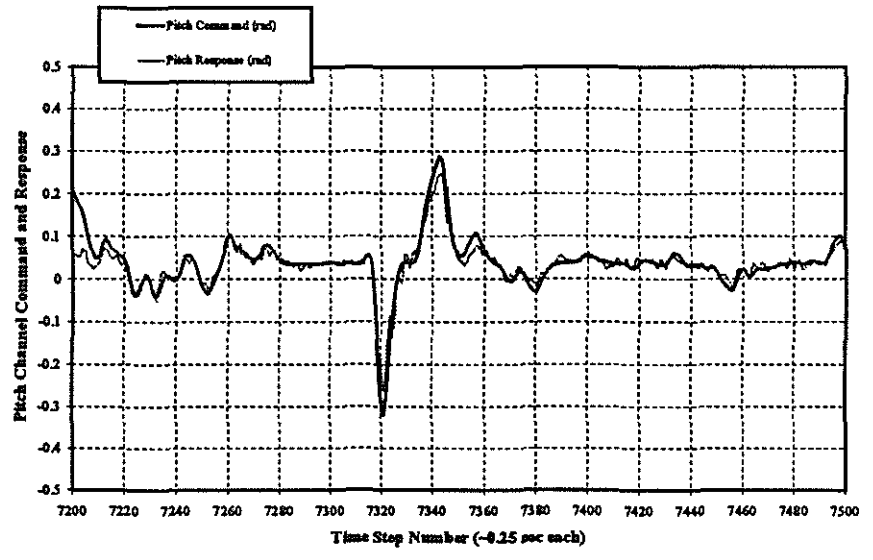

Figure 6. Pitch ACAH response for a doublet command, $\zeta = 0.8$, $\omega_n = 2.0$, with NN adaptation rate = 15.

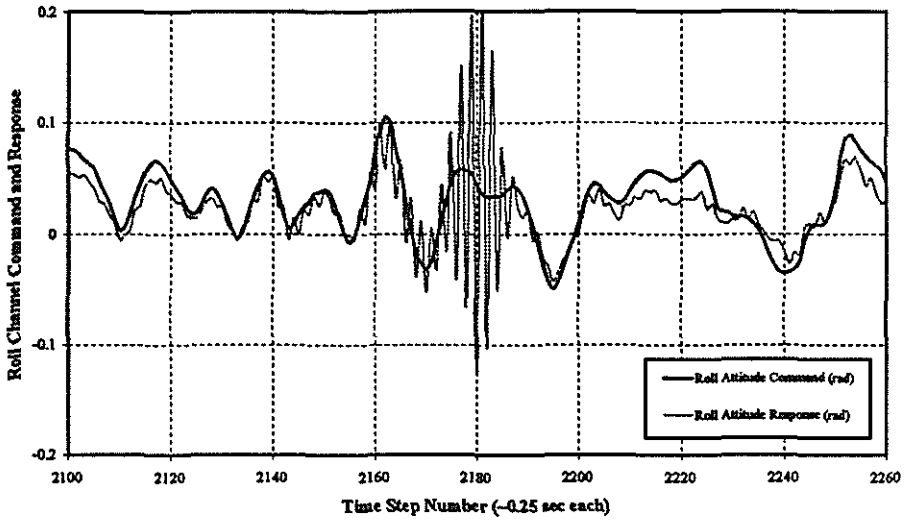

Figure 7. Roll ACAH response, $\zeta = 0.8$, ω_n is varied from 2 to 5 rad/sec, no neural network.

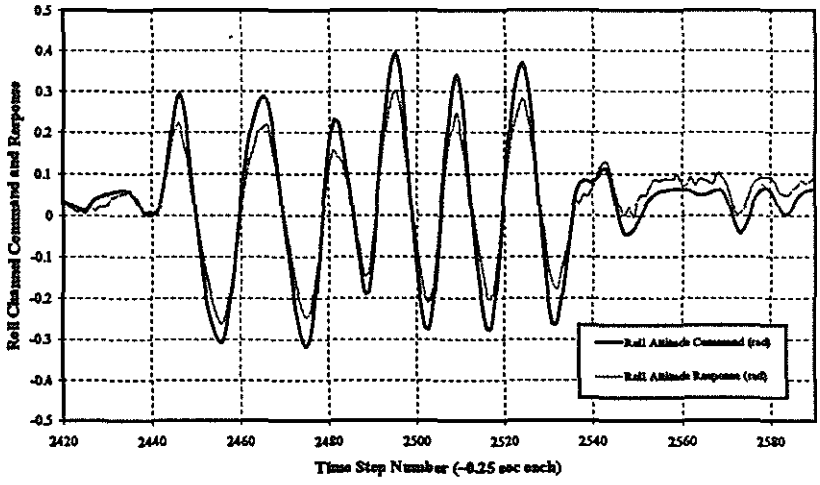

Figure 8. Roll ACAH response, $\zeta = 0.8$, $\omega_n = 3.5$ rad/sec, no neural network.

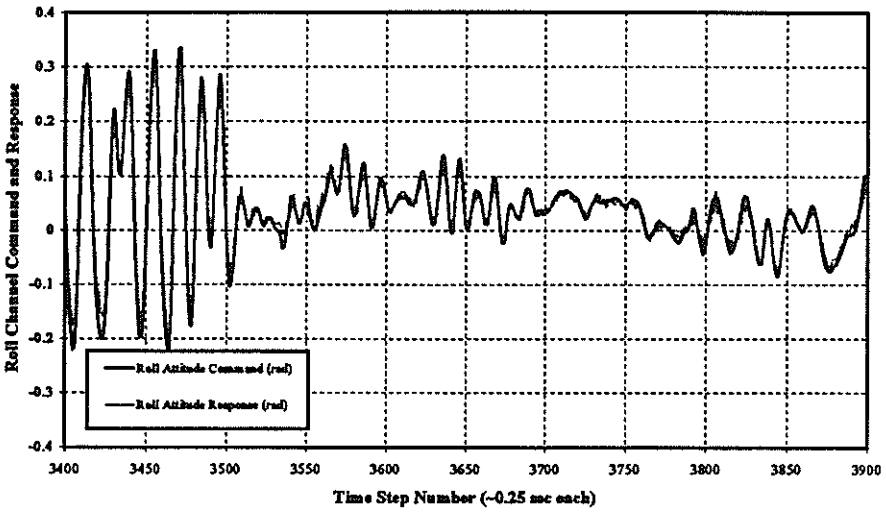

Figure 9. Roll ACAH response, $\zeta = 0.8$, $\omega_n = 3.5$ rad/sec, with neural network adaptation rate = 50.

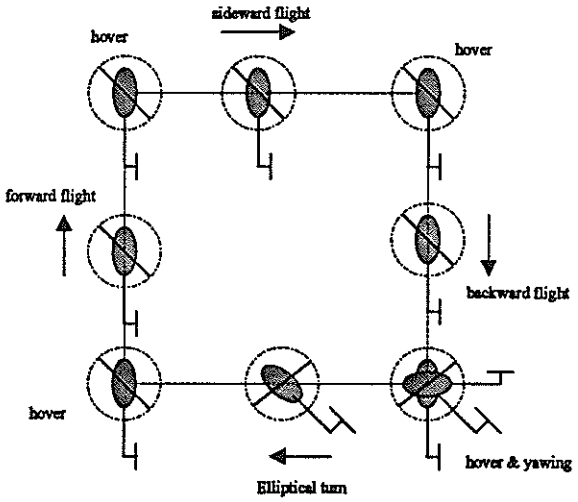

Figure 10. A sketch of the trajectory command used in simulations.

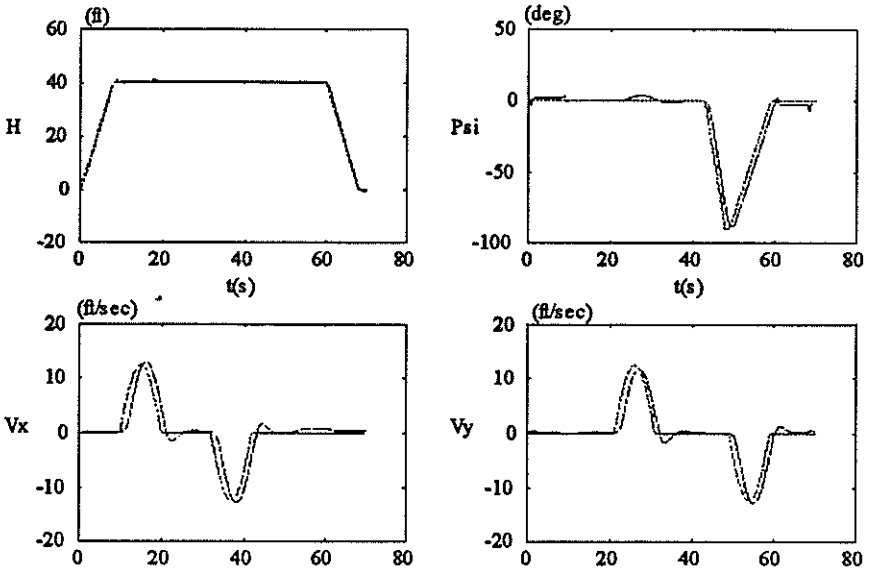

Figure 11. Variation of altitude (H), heading (psi), V_X and V_Y command and response.

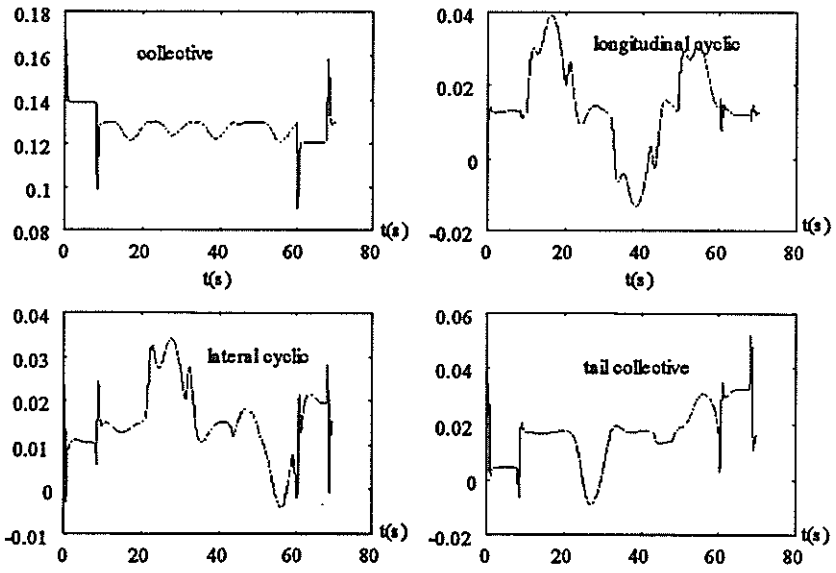

Figure 12. Control variations for trajectory command tracking.